# LEARNING TO PARALLEL: ACCELERATING DIFFUSION LARGE LANGUAGE MODELS VIA ADAPTIVE PARALLEL DECODING

**Anonymous authors**Paper under double-blind review

## **ABSTRACT**

Autoregressive decoding in large language models (LLMs) requires  $\mathcal{O}(n)$  sequential steps for n tokens, fundamentally limiting inference throughput. Recent diffusion-based LLMs (dLLMs) enable parallel token generation through iterative denoising. However, current parallel decoding strategies rely on fixed, input-agnostic heuristics (e.g., confidence thresholds), which fail to adapt to inputspecific characteristics, resulting in suboptimal speed-quality trade-offs across diverse NLP tasks. In this work, we explore a more flexible and dynamic approach to parallel decoding. We propose Learning to Parallel Decode (Learn2PD), a framework that trains a lightweight and adaptive filter model to predict, for each token position, whether the current prediction matches the final output. This learned filter approximates an oracle parallel decoding strategy that unmasks tokens only when correctly predicted. Importantly, the filter model is learned in a post-training manner, requiring only a small amount of computation to optimize it (minute-level GPU time). Additionally, we introduce End-of-Text Prediction (**EoTP**) to detect decoding completion at the end of sequence, avoiding redundant decoding of padding tokens. Experiments on the LLaDA [Nie et al., 2025] benchmark demonstrate that our method achieves up to 22.58x speedup without any performance drop, and up to 57.51× when combined with KV-Cache.

## 1 Introduction

Large Language Models (LLMs) [Zhao et al., 2023, Ziyu et al., 2023, Minaee et al., 2024] have demonstrated remarkable capabilities across a wide spectrum of natural language processing (NLP) tasks. However, most state-of-the-art LLMs rely on autoregressive (AR) decoding [Brown et al., 2020, Radford et al., 2019, Vaswani et al., 2017], which generates output tokens sequentially. Although this approach delivers strong generation quality, it inherently suffers from limited inference efficiency due to its strictly sequential nature [Leviathan et al., 2023, Stern et al., 2018]. To overcome this bottleneck, diffusion-based LLMs (dLLMs) [Nie et al., 2025, Ye et al., 2025] have been proposed as a compelling alternative by enabling parallel token generation through iterative denoising, potentially achieving sublinear complexity [Sohl-Dickstein et al., 2015, Li et al., 2022].

Diffusion-based LLMs (dLLMs) produce or iteratively refine the entire token sequence via denoising steps rather than predicting tokens one by one, so token-wise predictions at each step can be computed in parallel. Especially, most dLLMs adopt *semi-autoregressive decoding* [Arriola et al., 2025], which divides the target sequence into contiguous blocks and decodes the blocks from left to right. It facilitates token-parallelism by trading a small amount of autoregressive constraint for substantially higher parallel throughput, while still preserving essential left-to-right dependencies. To fully unlock these benefits, further development of a parallel decoding strategy that can leverage this approach is needed. Current methods employ static heuristics, for example, *confidence-based sampling* [Chang et al., 2022] prioritizes the most confident tokens for parallel decoding. Although these methods speed up inference, their static decoding strategies lead to poor generation quality.

Targeting this static limitation, we pose an intuitive question: *Instead of relying on a one-rule-fits-all decoding strategy, can we adopt a flexible, case-by-case one for parallel decoding?* To answer this, we analyzed the model's token-level decoding behavior and found that current models often remask

		GSM8K (5-shot) Generation Length=1024 Acc=77.6%
LLaDA	TPS: 0.54 tokens/s	
Learn2PD	TPS: 6.63 tokens/s	Acc = 77.3%
(Sec. 3.2)		12.21×
EoTP	TPS: 12.26 tokens/s	Acc = 79.8%
(Sec. 3.3)		22.58×
& KV Cache	TPS: 16.37 tokens/s	Acc = 74.0%
K v Cacile		57.51×

Figure 1: **Effectiveness of our proposed approaches.** We report the throughput and accuracy on GSM8K (5-shot, Generation Length=1024) with LLaDA and our proposed methods under four settings: (1) vanilla decoding, (2) Learn2PD policy, (3) Learn2PD and EoTP mechanism, (4) Learn2PD and EoTP integrated by KV Cache. Our proposed methods, Learn2PD and EoTP, yield a 22.58× speedup over the vanilla baseline while simultaneously preserving the original accuracy. Integration with KV Cache achieves a further improvement in throughput to 16.37 tokens/sec (a 57.51× speedup), with only a minimal loss in accuracy.

tokens that have already been correctly predicted, leading to unnecessary computational redundancy. Taking advantage of this finding, we propose that an effective parallel decoding strategy should be capable of eliminating such redundancy. To realize this goal, we first establish an oracle baseline: **Extremely Greedy Parallel (EGP)**, which unmasks each token immediately upon correct prediction. In the oracle, we use the reference answers to unmask a token when its prediction matches the ground truth. Our analysis reveals that this oracle can achieve a 15-20× speedup without quality loss, demonstrating substantial potential to improve parallel decoding. However, its dependence on unavailable ground truth makes it infeasible in practice.

To approximate this oracle, we propose **Learning to Parallel Decode** (**Learn2PD**), the first learned parallel decoding policy for dLLMs. The framework learns to predict when to finalize a token—that is, when we have sufficient confidence to accept its current prediction. The key insight is that diffusion models exhibit predictable confidence patterns [Song et al., 2020, Nichol & Dhariwal, 2021]: the confidence score for each token can be treated as an informative feature. Fluctuations in these scores capture the model's internal state of acceptance or doubt regarding its predictions. Specifically, we train a lightweight filter model  $f_{\theta}$  that predicts whether each token has been correctly generated. The filter model is optimized in the post-training phase, requiring minute-level GPU time for convergence. Once trained, this filter model remains fixed and requires no gradient updates during inference. The filter takes the model's confidence scores as input and outputs a binary decision for each token to indicate whether it should be remasked. Surprisingly, a simple two-layer MLP [Tolstikhin et al., 2021] performs exceptionally well at this task, as the block-level confidence patterns provide sufficient information for accurate convergence prediction, thus eliminating the need for complex architectures or task-specific feature engineering.

Another finding from the EGP oracle is that even when the [End-of-Text] token is unmasked, the model continues the decoding process for subsequent tokens. When the generation length is 1024, this inefficiency is responsible for 90% of the computational waste. To reduce the excessive decoding steps after the [End-of-Text] token, we introduce an **End-of-Text Prediction** (**EoTP**) mechanism. EoTP can terminate decoding as soon as the [End-of-Text] token is confidently generated, which avoids redundant computation and further boosts decoding efficiency.

Our method accelerates dLLMs by eliminating redundant decoding operations, thereby preserving generation quality. Experimental results demonstrate a remarkable 22.58× speed-up on LLaDA while fully maintaining its performance. Importantly, our method is **orthogonal** to existing optimizations: when combined with KV caching, the speedup compounds to 57.51× accompanied by only a slight degradation in accuracy (See Figure 1). In summary, our contributions are threefold:

- 1. We propose a novel and adaptive framework, **Learn2PD** that predicts which tokens have been correctly decoded, approximating the oracle Extremely Greedy Parallel Decoding strategy.
- 2. We also propose a **End-of-Text Prediction (EoTP)** mechanism to reduce the unnecessary decoding steps, which significantly boosts inference efficiency.
- 3. We extensively evaluate our method on various dLLMs across four representative benchmarks: GSM8K, MATH, HumanEval, and MBPP. Our method consistently achieves order-of-magnitude inference acceleration with negligible accuracy loss. Specifically, our method attains a significant 22.58× acceleration without any degradation in accuracy.

# 2 RELATED WORK

#### 2.1 DIFFUSION-BASED LARGE LANGUAGE MODELS

The integration of diffusion models with large language models (LLMs) is an emerging and promising direction in generative AI. Early work adapted continuous diffusion to discrete data domains [Sohl-Dickstein et al., 2015, Hoogeboom et al., 2021], leading to D3PM [Austin et al., 2021a], which introduced a Markov chain-based framework for discrete noise injection and denoising trained via ELBO maximization. This was extended to continuous time by CTMC [Campbell et al., 2022]. In parallel, SEDD [Lou et al., 2023] learned the reverse process by modeling the ratio of marginal probabilities using a denoising score entropy objective, while Masked Diffusion Models such as MDLM [Shi et al., 2024, Sahoo et al., 2024, Zheng et al., 2024] and RADD Ou et al. [2025] provided further theoretical simplifications and formalized connections between parameterizations. A key breakthrough has been the incorporation of diffusion into existing LLM architectures: Diffusion-NAT [Zhou et al., 2023] aligned the denoising process with non-autoregressive decoding, enabling high-speed generation, while models like LLaDA [Nie et al., 2025], DiffuLLaMA [Gong et al., 2025], and Dream [Ye et al., 2025] successfully scaled diffusion-based decoding to billion-parameter models, significantly improving inference efficiency without compromising output quality.

#### 2.2 ACCELERATE DIFFUSION-BASED LARGE LANGUAGE MODELS

Followed by mature diffusion large language models, their acceleration methods are also under development. Concretely, dllm-Cache [Liu et al., 2025] proposes a training-free, adaptive caching framework that performs long-interval prompt caching and short-interval, value-similarity-guided partial response updates. Fast-dLLM [Wu et al., 2025] introduces block-wise approximate KV caching and a confidence-aware parallel decoding rule that only decodes tokens whose marginal confidence exceeds a threshold. Hu et al. [2025] propose FreeCache to approximate KV states by reusing stable prompt/block activations across steps. They also introduce Guided Diffusion to decide which tokens to unmask each step without retraining. SlowFast-Sampling [Wei et al., 2025] proposes a dynamic two-stage sampler that alternates a cautious exploratory phase with a fast phase that aggressively decodes high-confidence tokens within that span. Prophet [Li et al., 2025] monitors the top-2 logit gap and commits all remaining tokens in one shot via early-commit decoding once it is sufficiently confident. However, these accelerate methods are often static and lack flexibility. To address this, we propose **Learn2PD**, a novel dynamic remasking method that achieves more efficient inference acceleration by reducing the unnecessary and repetitive decoding steps. Moreover, we also introduce EoTP to avoid redundant decoding when the answer does not span the full generation length.

#### 3 METHODOLOGY

In this section, we present Learn2PD, a learned approach to accelerate diffusion language model inference through adaptive parallel decoding. We begin by reviewing the fundamentals of diffusion language models and their current parallel decoding strategies (Section 3.1.1). Through empirical analysis, we reveal a critical inefficiency: existing methods unnecessarily remask a significant proportion of correctly predicted tokens, leading to redundant computation (Section 3.1.2). This observation motivates our core contribution—training a lightweight filter model to predict token stability and approximate an oracle parallel decoding strategy (Section 3.2). Finally, we introduce an early-stopping mechanism to further eliminate padding token overhead (Section 3.3)

## 3.1 PRELIMINARY

## 3.1.1 DIFFUSION LARGE LANGUAGE MODELS

**Forward Process.** Given an input sentence  $x_0 \in \{0, 1, ..., V-1\}^L$  and a noise level  $t \in [0, 1]$ , where V and L represent the vocabulary size and sentence length. The forward process randomly

and independently masks out tokens through the following Markov chain:

$$q_{t|0}(\boldsymbol{x}_t \mid \boldsymbol{x}_0) = \prod_{i=0}^{L-1} \left[ (1-t) \mathbf{1} \{ \boldsymbol{x}_t^i = \boldsymbol{x}_0^i \} + t \cdot \mathbf{1} \{ \boldsymbol{x}_t^i = m \} \right]$$
(1)

where  $x^i$  denotes the *i*-th element of x, m denotes the mask token [Devlin et al., 2019],  $x_t$  denotes the noisy data at time t, and  $q_0(\cdot)$  is the data distribution  $p_{\text{data}}(\cdot)$ .

**Reverse process.** The reverse process iteratively recovers masked tokens by predicting data distribution from a masked sequence. Transitioning from corruption level t to an earlier level s, where  $0 \le s < t \le 1$  can be approximated as

$$q_{s|t}(\boldsymbol{x}_{s} \mid \boldsymbol{x}_{t}) = \prod_{i=0}^{L-1} q_{s|t}(\boldsymbol{x}_{s}^{i} \mid \boldsymbol{x}_{t}), q_{s|t}(\boldsymbol{x}_{s}^{i} \mid \boldsymbol{x}_{t}) = \begin{cases} 1, & \boldsymbol{x}_{t}^{i} \neq m, \ \boldsymbol{x}_{s}^{i} = \boldsymbol{x}_{t}^{i}, \\ \frac{s}{t}, & \boldsymbol{x}_{t}^{i} = m, \ \boldsymbol{x}_{s}^{i} = m, \\ \frac{t-s}{t} \ q_{0|t}(\boldsymbol{x}_{s}^{i} \mid \boldsymbol{x}_{t}), & \boldsymbol{x}_{t}^{i} = m, \ \boldsymbol{x}_{s}^{i} \neq m, \end{cases}$$

where m represent the [MASK] and  $q_{0|t}(\cdot)$  is the data prediction distribution by the model [Ho et al., 2020]. Given a prompt  $c = (c_1, ..., c_M)$ , the response y is generated in K discrete steps. In each step k, a mask predictor  $p_{\theta}$  takes  $\mathbf{y}^{(k)}$  as input and predicts the distribution of sequence. The estimate of the sequence  $\hat{\mathbf{y}}^{(0)}$  is generated via greedy decoding:

$$\hat{\boldsymbol{y}}^{(0)} = \arg\max_{\boldsymbol{y} \in \mathcal{T}} P_{\theta} \left( \boldsymbol{y} \mid \mathbf{c}, \mathbf{y}^{(k)} \right) = \arg\max_{\boldsymbol{y} \in \mathcal{T}} p_{\theta} \left( \mathbf{c}, \mathbf{y}^{(k)}; \theta \right)$$
(3)

**Low-Confidence Remasking.** To improve the sample quality, the unmasking tokens with low confidence would be remasked. This approach follows a common practice in non-autoregressive generation for improving output fidelity [Ghazvininejad et al., 2019]. For each position i, the model predicts  $\hat{y_0}^{(k)}$  and computes its confidence  $c_i$ , which is given by:

$$c_i = P_{\theta} \left( \hat{\mathbf{y}_{0,i}}^{(k)} \mid \mathbf{c}, \mathbf{y}^{(k)} \right) \tag{4}$$

The tokens corresponding to the n lowest confidence would be set to <code>[MASK]</code> again, where n is calculated by the noise level t.

## 3.1.2 Unnecessary repetitive decoding

Building on the iterative inference process displayed in Section 3.1.1, we investigate the unnecessary and repetitive decoding conditions in diffusion-based large language models. We conducted experimental analyses with LLaDA-8B-Instruct[Nie et al., 2025] on two widely used datasets: GSM8K [Cobbe et al., 2021] and HumanEval [Chen et al., 2021]. We choose LLaDA as our base model due to its state-of-the-art performance and availability of pre-trained checkpoints across multiple scales. Specifically, we measured the amount of unnecessary and repetitive decoding, which is defined as the number of times the model continues to decode a token after that token has first matched the reference answer. In this paper, we refer to the answer produced by LLaDA under the standard generation process as the reference answer.

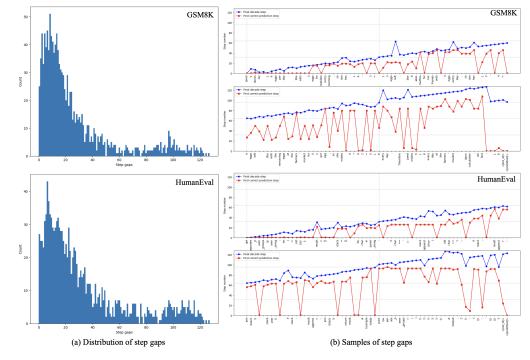


Figure 2: The unnecessary and repetitive decoding steps in different datasets: GSM8K and HumanEval. (a) Distributions of gaps. These two histograms show the distribution of step gaps for each token between the decoding step and the step with the first correct prediction. (b) Samples of gaps. The red line means the first correct prediction step, and the blue line means the actual decoding step.

<sup>&</sup>lt;sup>1</sup>For all analyses in this section, we set LLaDA's Generation Length at 128 and Block Size at 32.

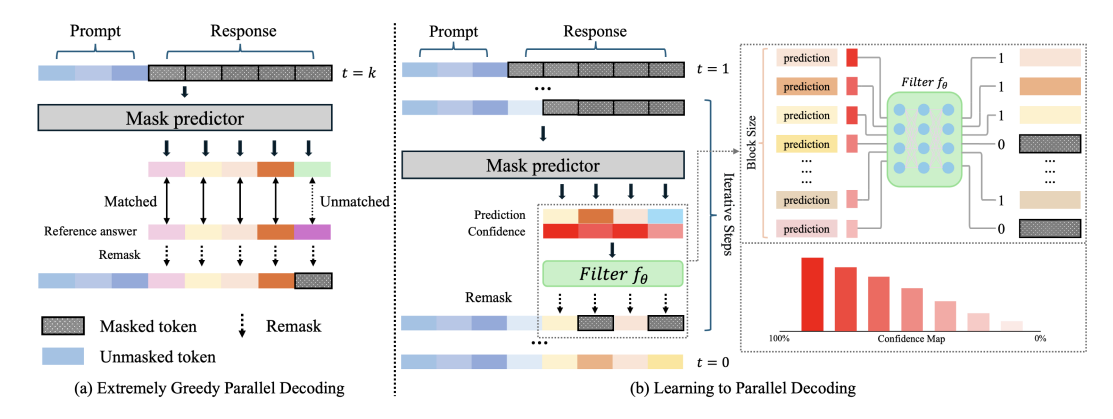


Figure 3: A Conceptual Overview of pipeline and method. (a) Extremely Greedy Parallel (EGP). This strategy compares the predicted tokens with the reference answer and only remasks the tokens that do not match in these comparisons. (b) Learning to Parallel Decoding (Learn2PD). During the inference process, after the model generates predictions and confidences for each token, the confidence of each token is fed into a filter model  $f_{\theta}$  to determine which tokens need to be remasked. This determination then guides the subsequent remasking procedure.

**Analysis of unnecessary repetition.** As illustrated in Figure 2 (a), we tally up the distribution of the step gaps between the decoding step and the step with the first correct prediction. For each dataset, we randomly sample 10 questions to conduct the experiment. We find that most of the tokens still need to be decoded more than 10 times, even though they are already correct. And Figure 2 (b) shows one sample from each dataset. The red line means the first correct prediction step, and the blue line means the actual decoding step. It is clear that the model performs many unnecessary decoding steps before unmasking the tokens.

## 3.1.3 EXPECTED INFERENCE PROCESS: EXTREMELY GREEDY PARALLEL (EGP)

Based on the above findings, we observe that a large portion of tokens are remasked as [MASK] and decoded multiple times even after they have already been decoded to the reference answer. Motivated by this, we define the **Extremely Greedy Parallel (EGP)** oracle as: at each step k, unmask token i if and only if  $M(x^k)_i = y_i$ , where  $y_i$  is the reference answer for token i. This oracle achieves optimal speedup by never remasking correct predictions.

Acceleration Potential. To evaluate the efficiency of our strategy, we compared the number of decoding steps required per block for LLaDA-8B-Instruct on the GSM8K dataset under the Extremely Greedy Parallel policy versus the standard decoding regime. Similarly, we fix the Generation Length to 256 and the Block Size to 32.

As shown in Figure 4, the results are striking. Our strategy achieves a median of 2 decodings per block while maintaining the same accuracy. In contrast, LLaDA with the vanilla setting requires 32 decodings per block. This demonstrates a substantial opportunity for efficiency gains, without compromising output quality.

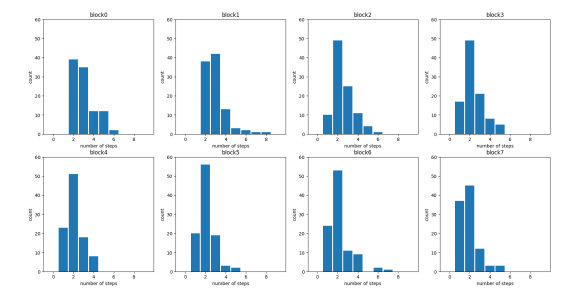


Figure 4: **Distribution of decoding steps per block with Extremely Greedy Parallel (EGP) strategy.** Histograms illustrate the number of decoding steps performed in each block when using our strategy with LLaDA-8B-Instruct on GSM8K based on 100 samples.

#### 3.2 Learning to Parallel Decoding

Although our Extremely Greedy Parallel strategy performs well, this oracle requires ground truth tokens that are unavailable during inference. To address this, we propose a novel approach: **Learning to Parallel Decoding** (**Learn2PD**). Our goal is to simulate the EGP strategy after each decoding step to select tokens and decide whether to remask. We can reformulate this as an optimization problem by using Binary Cross-Entropy Loss (BCELoss) [De Boer et al., 2005]:

$$\arg\min -\frac{1}{m} \sum_{i=1}^{m} \left[ y_i \log p_i + (1 - y_i) \log(1 - p_i) \right]$$
 (5)

where  $y_i$  indicates whether token  $t_i$  should be remasked under the EGP strategy: 0 means it should be remasked and 1 means it can be unmasked. During the inference process, a threshold  $\tau$  is applied to discretize  $p_i$  into either 0 or 1. The  $p_i$  is generated from which we called the filter model  $f_{\theta}$ . In this algorithm, the only trained parameters are  $\theta$ . Therefore, the parameters of the diffusion large language model remain unchanged. Then, the training loss should be:

$$\mathcal{L}_{BCE} = -\frac{1}{m} \sum_{i=1}^{m} \left[ y_i \log \sigma(z_i) + (1 - y_i) \log(1 - \sigma(z_i)) \right]$$
 (6)

where  $z_i$  is the output of the filter model (logit). We show the algorithms for training and inference in Algorithm 1 and Algorithm 2. The filter  $f_{\theta}$  takes the confidence of the prediction as input and returns the logits z to indicate the probability of no remask. And in order to ensure z remains in the range [0,1], we apply a sigmoid function on z before it is passed to the dLLMs. Critically, the filter model  $f_{\theta}$  adds negligible overhead during inference. Our experimental results in Section 4 quantitatively demonstrate that the achieved speedup vastly outweighs this minimal overhead.

#### **Algorithm 1** Training

270

271

272

273274

275

276

277278

279

280 281

282

283

284

285

287 288 289

290

291

292

293

295

296

297

298

299

300

301

302

303

304

305 306

307

308

310

311

312

313

314

315

316

317

318

319

320

321

322

323

```
Require: Diffusion large language model M, filter model f_{\theta}, prompt set x_{\text{prompt}}, reference answer set x_{\text{reference}}, generation length L_{\text{gen}}, learning rate \eta, block size s
```

```
repeat
2:
           x_i \in x_{\text{prompt}}, r_i \in x_{\text{reference}}, l_i = length(x_i)
           X \leftarrow \mathrm{concat}(x_{\underline{i}}, [\mathrm{MASK}]^{L_{\mathrm{gen}}})
3:
           for b=0,...,\frac{L_{\mathrm{gen}}}{s}-1 do
4:
5:
                  \mathcal{M} \leftarrow \{1, 2, ..., s\}
6:
7:
8:
                  while \mathcal{M} \neq \emptyset do
                        conf_t, pre_t = M(X)
                        if pre_{t,j} = r_{i,j} then
9:
                              \hat{y_j} \leftarrow 1, \mathcal{M} \leftarrow \mathcal{M} \setminus \{j\}
10:
                                X_{l_i+b\cdot s+j} \leftarrow pre_{t,j}
11:
12:
13:
                          end if
                          \mathcal{L} \leftarrow BCELoss(\hat{y}, f_{\theta}(conf_t))
                         \theta \leftarrow \theta - \eta \cdot \nabla_{\theta} L
15:
16:
                    end while
              end for
18: until converged
```

# Algorithm 2 Inference

**Require:** Diffusion large language model M, filter model  $f_{\theta}$ , prompt set  $x_{\text{prompt}}$ , generation length  $L_{\text{gen}}$ , block size s, filter threshold  $\tau$ 

```
for each x_i \in x_{\text{prompt}} do
2:
           l_i = \operatorname{length}(x_i), X \leftarrow \operatorname{concat}(x_i, [MASK]^{L_{gen}})
           for b=0,...,\frac{L_{\mathrm{gen}}}{s}-1 do
3:
4:
                \mathcal{M} \leftarrow \{1, 2, ..., s\}
5:
                while \mathcal{M} \neq \emptyset do
6:
                      conf_t, pre_t = M(X), logit_t = f_\theta(conf_t)
7:
                      if \operatorname{logit}_{t,j} > \tau then
8:
                           \mathcal{M} \leftarrow \mathcal{M} \setminus \{j\}, X_{i+b \cdot s+j} \leftarrow \operatorname{pre}_{t,j}
9:
                      end if
10.
                  end while
11:
            end for
12:
            response_i = X_{l_i:l_i+L_{gen}-1}
13: end for
14: return response
```

#### 3.3 END-OF-TEXT PREDICTION

Besides the methods mentioned earlier, we observed that when the generation length of a diffusion large language model is increased to 1024, the generation time rises significantly for the same question compared to a length of 256, even though the final answer length remains unchanged. According to the analysis of the generated output, we find that the extra length is filled with the [EoT] token, and the additional decoding time is spent repeatedly decoding the [EoT] token. Based on this, we propose the **End-of-Text Prediction** (**EoTP**) approach: whenever the last decoded token is [EoT], the model would terminate the decoding process immediately and return the response. Therefore, we update the inference process to handle the long generation length challenge in Appendix B. Our analysis shows that 89.59% of

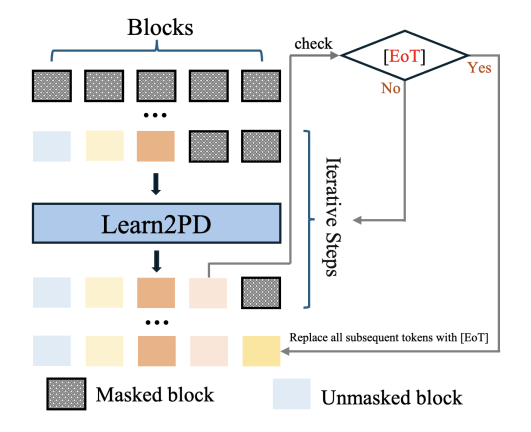


Figure 5: Schematic of the End-of-Text Prediction Policy. During the inference process, upon detection of an [EoT] token in a decoded block, all subsequent tokens are assigned with [EoT], and the inference is halted immediately.

Table 1: Benchmark results on the LLaDA-8B-Instruct suite. Each method was evaluated using two generation lengths (128 and 1024) across four datasets. Performance is measured using three metrics: TPS (tokens/sec), speedup, and accuracy score. The highest throughput and speedup values for each configuration are highlighted in bold.

Task	Methods	Gen Length	Inference Efficiency		Performance
lask			TPS↑	Speed (TPS)↑	Score
	LLaDA-8B-Instruct	256	3.41	1.00×	78.70
	LLaDA-ob-instruct	1024	0.54	1.00×	77.60
GSM8K	+ Learn2PD	256	$14.07_{+10.66}$	4.13×	78.62
(5-shot)		1024	$6.63_{+6.09}$	12.21×	77.26
	Learn2PD + EoTP	256	$14.35_{+10.94}$	4.21×	78.62
		1024	$12.26_{+11.72}$	22.58×	79.83
	LLaDA-8B-Instruct	256	4.70	1.00×	32.90
		1024	1.70	1.00×	35.21
Math	+ Learn2PD	256	$15.16_{+10.46}$	3.21×	32.22
(4-shot)		1024	$10.98_{+9.28}$	6.45×	34.01
	Learn2PD + EoTP	256	$15.21_{+10.51}$	3.23×	31.40
		1024	$12.27_{+10.57}$	<b>7.22</b> ×	34.60
	LLaDA-8B-Instruct	256	3.33	1.00×	39.63
		1024	0.53	1.00×	37.21
HumanEval	+ Learn2PD	256	11.66+8.33	3.5×	38.41
(0-shot)		1024	$4.63_{+4.10}$	8.78×	37.84
	Learn2PD + EoTP	256	11.88+8.55	3.57×	38.41
		1024	$6.63_{+6.10}$	12.55×	35.98
	LLaDA-8B-Instruct	256	3.14	1.00×	31.22
		1024	0.58	1.00×	10.61
MBPP	+ Learn2PD	256	$14.96_{+11.82}$	4.77×	30.84
(3-shot)	T Lealii2i D	1024	$6.96_{+6.38}$	12.08×	10.04
	Learn2PD + EoTP	256	$15.88_{+12.74}$	5.06×	31.03
		1024	$9.89_{+9.31}$	17.16×	11.02

computational cost comes from decoding padding tokens after <code>[EoT]</code>. EoTP eliminates this overhead by detecting sequence completion when all non-<code>[MASK]</code> positions have unmasked. The experiments and relevant analysis are in Appendix C.

## 4 EXPERIMENT

## 4.1 EXPERIMENTAL SETTINGS

**Models and Datasets.** We implement our methods on the representative dLLM: LLaDA-8B-Instruct [Nie et al., 2025] to measure the acceleration of the inference process across various benchmarks. To ensure the broad applicability of the methods, we conducted experiments on four datasets covering three different types of problems, which are GSM8K[Cobbe et al., 2021], Math [Lewkowycz et al., 2022], HumanEval[Chen et al., 2021], and MBPP [Austin et al., 2021b]. All experiments are conducted on 4 NVIDIA A6000 GPUs.

**Filter Model**  $f_{\theta}$  **Training.** To train a filter model that can be applied to a wide range of tasks, we selected 40 samples from each of the 66 types of questions in the FLAN dataset, resulting in a total of 2,640 samples for training. In this experiment, we used the simplest two-layer MLP as our filter model. Since the dLLMs remains frozen and only  $f_{\theta}$  is trained, the number of trainable parameters is extremely limited. For example, for an LLaDA with a block size of 32, the total number of trainable parameters is only 2,112. We trained  $f_{\theta}$  for 5,000 epochs until the model converged. The learning rate is set to 0.001, and the AdamW optimizer is used to optimize  $f_{\theta}$ .

Our training process consists of two stages. In the first stage, samples are collected by following an Extremely Greedy Parallel policy, recording the confidence scores and token selections at each step during parallel decoding. This data is then used in the second stage to train a filter model  $f_{\theta}$ . The data collection in the first stage was conducted on 4 NVIDIA RTX A6000 GPUs and took approximately three hours. The subsequent training of the filter model in the second stage was deployed on a T4 GPU and required only 6 minutes. The details of training are in Appendix D.

**Evaluation.** We evaluate the inference acceleration and generation quality of **Learn2PD** and **EoTP** methods by using quantitive metrics. The inference speed is quantified with Tokens Per Second (TPS), indicating the average number of tokens generated per second. And the generation quality is measured in task-specific metrics, such as accuracy for GSM8K, showing the model's performance with acceleration methods. In addition to this, we set the Generation Length to 256 & 1024 and the Block Size to 32.

#### 4.2 MAIN RESULTS

378

379

380

381

382

383 384

385

386

387

388

389

390 391

392 393

394

396

397

398

399

400

401

402

403

404 405

406 407

408

409

410

411

412

413

414

415

416 417

418

419

420

421

422

423 424

430

431

We present the inference performance and efficiency profits for Learn2PD and EoTP on the LLaDA-8B-Instruct across four benchmarks, as shown in Table 1.

In summary, Learn2PD significantly enhances inference efficiency across all tasks. Compared to the baseline model, our optimal method typically achieves a 3 to 4 times speedup at a generation length of 256 and a 6 to 12 times speedup at a generation length of 1024. When EoTP is incorporated, the improvements become even more pronounced, particularly with a generation length of 1024. For instance, combining Learn2PD and EoTP results in a throughput increase of 22.58x (on GSM8K, 5-shot) and 17.16× (on MBPP, 3-shot) relative to the baseline. These results demonstrate that our methods are not only effective individually but also highly orthogonal, resulting in compounded acceleration. More importantly, these efficiency gains have negligible impact on accuracy. The performance scores of our accelerated methods remain within 1–2 points of the baseline, and in some cases, the score is even slightly improved.

## 4.3 COMPATIBILITY WITH KEY-VALUE CACHE

We further evaluate the compatibility of our approach with established Key-Value (KV) Cache techniques by integrating both Dual Cache and Prefix Cache strategies [Wu et al., 2025]. Experiments are conducted on GSM8K with a generation length of 1024 tokens. As summarized in Table 2, the baseline model (Learn2PD & EoTP) achieves a throughput of 12.26 TPS, a speed-up of 22.58×, and an accuracy score of 79.83. When augmented with the Dual Cache, the system attains substantially higher efficiency, reaching 31.23 TPS and a 57.51× speedup, albeit with a slight decrease in accuracy (74.00). Similarly, incorporating the Prefix Cache also brings noticeable improvements, yielding 14.79 TPS and a 27.23× acceleration while maintaining a competitive score of 77.71. These results confirm that our method is orthogonal to and fully compatible with standard KV caching mechanisms, demonstrating its ability to leverage such strategies to enhance inference efficiency.

patible with existing KV caching strategies.

Methods	TPS	Speed	Score
Learn2PD & EoTP	12.26	$22.58 \times$	79.83
+ Dual Cache	31.23	$57.51 \times$	74.00
+ Prefix Cache	14.79	$27.23 \times$	77.71

Table 2: A comparison of our method with and Table 3: A comparison of the acceleration perforwithout KV Cache. The results show a signifi- mance using filter models of varying complexcant performance improvement when augmented ity (represented by the number of MLP layers). with both Dual and Prefix Caches, underscoring The results indicate that a two-layer MLP model that our method is orthogonal to and fully com- achieves the optimal balance by providing significant speedup.

# Layers	TPS	Speed	Score
Single-layer	8.77	$2.57\times$	78.62
Two-layer	14.07	$4.13\times$	78.62
Four-layer	11.41	$3.35 \times$	78.85

## 4.4 ANALYSIS: ABLATION STUDY

**Effect of Filter Model**  $f_{\theta}$  **Complexity.** To investigate the impact of the filter model's architectural complexity on acceleration performance, we conduct an ablation study using MLP-based fil-

433

434

435

436

437

438 439

440

441

442

443

444

445

446

447

448

449

450

451

452

453

454

455 456

457

458

459

460

461

462

463

464

465

466

467

468

469

470

471

472

473 474

475 476

477

478

479

480

481

482

483

484

485

ter models with varying depths. As illustrated in Table 3, a two-layer MLP achieves the highest throughput (14.07 TPS) and speed-up (4.13×), while maintaining 78.62% accuracy. In comparison, the single-layer model yields lower efficiency with a similar accuracy, suggesting limited representational capacity. Although the four-layer model attains a marginally better accuracy score, it results in reduced inference speed, indicating increased computational overhead. These results demonstrate that a two-layer configuration offers the optimal trade-off between efficiency and predictive performance, effectively balancing model complexity and acceleration gain.

**Effect of Generation Length.** To examine the impact of generation length on the performance of our methods, we compare the speedup and accuracy of Learn2PD and its enhanced variant (Learn2PD & EoTP) across varying output lengths. As shown in Table 4, both methods achieve greater acceleration as the generation length increases, while consistently maintaining competitive scores. At a shorter length of 128, Learn2PD & EoTP reaches a speed-up of 3.36x. And the speed-up improves steadily with longer sequences, culminating in a substantial 22.58× acceleration at a length of 1024. These results indicate that our approach is particularly effective for long-sequence generation, efficiently reducing the unnecessary decodings to maximize inference speed without compromising output quality.

**Effect of Filter Model**  $f_{\theta}$  **threshold**  $\tau$ **.** We perform an ablation study to examine the impact of the filtering threshold on inference accuracy and throughput. As shown in Figure 6, reducing the threshold improves throughput but leads to a corresponding decline in accuracy. For example, at  $\tau = 0.99$ , the model achieves a throughput of 4.68 TPS (vs. baseline 3.41 TPS) with 78.92% accuracy. In contrast, lowering the threshold to  $\tau = 0.9$  causes a more pronounced reduction in accuracy. The results indicate that a threshold of  $\tau = 0.96$  offers an optimal balance, delivering both high throughput (4.13× speedup) and near-baseline accuracy. These findings underscore the critical role of the filtering threshold in achieving an effective trade-off between inference efficiency and output quality.

Table 4: Performance comparison of our methods across different generation lengths. While maintaining a comparable accuracy, both Learn2PD and EoTP deliver substantially greater speedup at a length of 1024 compared to shorter sequences.

Gen Length	Methods	Speed	Score
128	Learn2PD	3.29×	73.92
	Learn2PD & EoTP	3.36×	74.07
256	Learn2PD	4.13×	78.62
	Learn2PD & EoTP	4.21×	78.62
512	Learn2PD	6.66×	77.71
	Learn2PD & EoTP	7.60×	79.68
1024	Learn2PD	12.21×	77.26
	Learn2PD & EoTP	22.58×	79.83

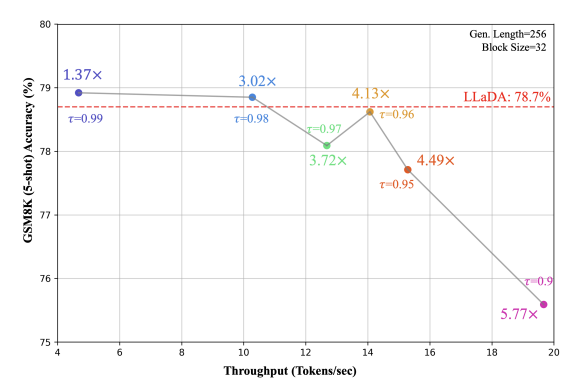


Figure 6: Impact of the filtering threshold on accuracy and throughout. We find that a threshold of 0.96 represents a favorable balance, maintaining high accuracy and comparable inference speed.

#### 5 Conclusion

In this work, we investigate the issue of extensive repetitive decoding during inference in Diffusion-based Large Language Models. To enable timely unmasking of correctly predicted tokens, we propose **Learn2PD**, a parallel decoding architecture that employs a filter model to make case-specific selections. This filter model is lightweight and pre-trained, thus requiring no additional training during inference. Furthermore, to address the time overhead caused by repeated encoding of the  $[E \circ T]$  token as the generation length increases, we introduce the **EoTP** mechanism, which halts decoding immediately after  $[E \circ T]$  is generated, thereby reducing unnecessary computational cost. Extensive experiments across multiple benchmarks and model baselines (LLaDA) demonstrate that our approach achieves up to **22.58**× speedup without sacrificing accuracy—and up to **57.51**× when combined with KV Cache. Our proposed method offers a compelling solution for deploying diffusion-based LLMs as alternatives to autoregressive models in future applications.

# ETHICS STATEMENT

Potential for Misuse: We acknowledge that our acceleration techniques, by lowering the computational cost of inference, could inadvertently lower the barrier for malicious use. This could enable bad actors to scale up harmful applications such as disinformation campaigns, spam, phishing, or automated malicious code generation more efficiently.

## REPRODUCIBILITY STATEMENT

To support reproducibility, a complete anonymized code repository is provided as supplementary material. The repository encompasses all necessary components to replicate our work: the implementation source code for the proposed model and algorithms, the scripts required to run the experiments, comprehensive hyperparameter configuration files, and detailed execution instructions.

## REFERENCES

- Marianne Arriola, Subham Sekhar Sahoo, Aaron Gokaslan, Zhihan Yang, Zhixuan Qi, Jiaqi Han, Justin T Chiu, and Volodymyr Kuleshov. Block diffusion: Interpolating between autoregressive and diffusion language models. In *The Thirteenth International Conference on Learning Representations*, 2025. URL https://openreview.net/forum?id=tyEyYT267x.
- Jacob Austin, Daniel D Johnson, Jonathan Ho, Daniel Tarlow, and Rianne Van Den Berg. Structured denoising diffusion models in discrete state-spaces. *Advances in neural information processing systems*, 34:17981–17993, 2021a.
- Jacob Austin, Augustus Odena, Maxwell Nye, Maarten Bosma, Henryk Michalewski, David Dohan, Ellen Jiang, Carrie Cai, Michael Terry, Quoc Le, et al. Program synthesis with large language models. arXiv preprint arXiv:2108.07732, 2021b.
- Tom Brown, Benjamin Mann, Nick Ryder, Melanie Subbiah, Jared D Kaplan, Prafulla Dhariwal, Arvind Neelakantan, Pranav Shyam, Girish Sastry, Amanda Askell, et al. Language models are few-shot learners. *Advances in neural information processing systems*, 33:1877–1901, 2020.
- Andrew Campbell, Joe Benton, Valentin De Bortoli, Thomas Rainforth, George Deligiannidis, and Arnaud Doucet. A continuous time framework for discrete denoising models. *Advances in Neural Information Processing Systems*, 35:28266–28279, 2022.
- Huiwen Chang, Han Zhang, Lu Jiang, Ce Liu, and William T. Freeman. Maskgit: Masked generative image transformer. In *The IEEE Conference on Computer Vision and Pattern Recognition (CVPR)*, June 2022.
- Mark Chen, Jerry Tworek, Heewoo Jun, Qiming Yuan, Henrique Ponde de Oliveira Pinto, Jared Kaplan, Harri Edwards, Yuri Burda, Nicholas Joseph, Greg Brockman, Alex Ray, Raul Puri, Gretchen Krueger, Michael Petrov, Heidy Khlaaf, Girish Sastry, Pamela Mishkin, Brooke Chan, Scott Gray, Nick Ryder, Mikhail Pavlov, Alethea Power, Lukasz Kaiser, Mohammad Bavarian, Clemens Winter, Philippe Tillet, Felipe Petroski Such, Dave Cummings, Matthias Plappert, Fotios Chantzis, Elizabeth Barnes, Ariel Herbert-Voss, William Hebgen Guss, Alex Nichol, Alex Paino, Nikolas Tezak, Jie Tang, Igor Babuschkin, Suchir Balaji, Shantanu Jain, William Saunders, Christopher Hesse, Andrew N. Carr, Jan Leike, Josh Achiam, Vedant Misra, Evan Morikawa, Alec Radford, Matthew Knight, Miles Brundage, Mira Murati, Katie Mayer, Peter Welinder, Bob McGrew, Dario Amodei, Sam McCandlish, Ilya Sutskever, and Wojciech Zaremba. Evaluating large language models trained on code. 2021.
- Karl Cobbe, Vineet Kosaraju, Mohammad Bavarian, Mark Chen, Heewoo Jun, Lukasz Kaiser, Matthias Plappert, Jerry Tworek, Jacob Hilton, Reiichiro Nakano, Christopher Hesse, and John Schulman. Training verifiers to solve math word problems. *arXiv preprint arXiv:2110.14168*, 2021.
- Pieter-Tjerk De Boer, Dirk P Kroese, Shie Mannor, and Reuven Y Rubinstein. A tutorial on the cross-entropy method. *Annals of operations research*, 134(1):19–67, 2005.

- Jacob Devlin, Ming-Wei Chang, Kenton Lee, and Kristina Toutanova. Bert: Pre-training of deep bidirectional transformers for language understanding. In *Proceedings of the 2019 conference of the North American chapter of the association for computational linguistics: human language technologies, volume 1 (long and short papers)*, pp. 4171–4186, 2019.
- Marjan Ghazvininejad, Omer Levy, Yinhan Liu, and Luke Zettlemoyer. Mask-predict: Parallel decoding of conditional masked language models. *arXiv preprint arXiv:1904.09324*, 2019.
- Shansan Gong, Shivam Agarwal, Yizhe Zhang, Jiacheng Ye, Lin Zheng, Mukai Li, Chenxin An, Peilin Zhao, Wei Bi, Jiawei Han, Hao Peng, and Lingpeng Kong. Scaling diffusion language models via adaptation from autoregressive models. In *The Thirteenth International Conference on Learning Representations*, 2025. URL https://openreview.net/forum?id=jltSLYKwg8.
- Jonathan Ho, Ajay Jain, and Pieter Abbeel. Denoising diffusion probabilistic models. *Advances in neural information processing systems*, 33:6840–6851, 2020.
- Emiel Hoogeboom, Didrik Nielsen, Priyank Jaini, Patrick Forré, and Max Welling. Argmax flows and multinomial diffusion: Learning categorical distributions. *Advances in neural information processing systems*, 34:12454–12465, 2021.
- Zhanqiu Hu, Jian Meng, Yash Akhauri, Mohamed S Abdelfattah, Jae-sun Seo, Zhiru Zhang, and Udit Gupta. Accelerating diffusion language model inference via efficient kv caching and guided diffusion. *arXiv preprint arXiv:2505.21467*, 2025.
- Yaniv Leviathan, Matan Kalman, and Yossi Matias. Fast inference from transformers via speculative decoding. In *International Conference on Machine Learning*, pp. 19274–19286. PMLR, 2023.
- Aitor Lewkowycz, Anders Johan Andreassen, David Dohan, Ethan Dyer, Henryk Michalewski, Vinay Venkatesh Ramasesh, Ambrose Slone, Cem Anil, Imanol Schlag, Theo Gutman-Solo, Yuhuai Wu, Behnam Neyshabur, Guy Gur-Ari, and Vedant Misra. Solving quantitative reasoning problems with language models. In Alice H. Oh, Alekh Agarwal, Danielle Belgrave, and Kyunghyun Cho (eds.), *Advances in Neural Information Processing Systems*, 2022. URL https://openreview.net/forum?id=IFXTZERXdM7.
- Pengxiang Li, Yefan Zhou, Dilxat Muhtar, Lu Yin, Shilin Yan, Li Shen, Yi Liang, Soroush Vosoughi, and Shiwei Liu. Diffusion language models know the answer before decoding. *arXiv* preprint *arXiv*:2508.19982, 2025.
- Xiang Li, John Thickstun, Ishaan Gulrajani, Percy S Liang, and Tatsunori B Hashimoto. Diffusion-lm improves controllable text generation. *Advances in neural information processing systems*, 35: 4328–4343, 2022.
- Zhiyuan Liu, Yicun Yang, Yaojie Zhang, Junjie Chen, Chang Zou, Qingyuan Wei, Shaobo Wang, and Linfeng Zhang. dllm-cache: Accelerating diffusion large language models with adaptive caching. arXiv preprint arXiv:2506.06295, 2025.
- Aaron Lou, Chenlin Meng, and Stefano Ermon. Discrete diffusion language modeling by estimating the ratios of the data distribution. 2023.
- Shervin Minaee, Tomas Mikolov, Narjes Nikzad, Meysam Asgari Chenaghlu, Richard Socher, Xavier Amatriain, and Jianfeng Gao. Large language models: A survey. *ArXiv*, abs/2402.06196, 2024. URL https://api.semanticscholar.org/CorpusID:267617032.
- Alexander Quinn Nichol and Prafulla Dhariwal. Improved denoising diffusion probabilistic models. In *International conference on machine learning*, pp. 8162–8171. PMLR, 2021.
- Shen Nie, Fengqi Zhu, Zebin You, Xiaolu Zhang, Jingyang Ou, Jun Hu, Jun Zhou, Yankai Lin, Ji-Rong Wen, and Chongxuan Li. Large language diffusion models. *arXiv preprint arXiv:2502.09992*, 2025.

Jingyang Ou, Shen Nie, Kaiwen Xue, Fengqi Zhu, Jiacheng Sun, Zhenguo Li, and Chongxuan Li. Your absorbing discrete diffusion secretly models the conditional distributions of clean data. In *The Thirteenth International Conference on Learning Representations*, 2025. URL https://openreview.net/forum?id=sMyXP8Tanm.

- Alec Radford, Jeffrey Wu, Rewon Child, David Luan, Dario Amodei, Ilya Sutskever, et al. Language models are unsupervised multitask learners. *OpenAI blog*, 1(8):9, 2019.
- Subham Sahoo, Marianne Arriola, Yair Schiff, Aaron Gokaslan, Edgar Marroquin, Justin Chiu, Alexander Rush, and Volodymyr Kuleshov. Simple and effective masked diffusion language models. *Advances in Neural Information Processing Systems*, 37:130136–130184, 2024.
- Jiaxin Shi, Kehang Han, Zhe Wang, Arnaud Doucet, and Michalis Titsias. Simplified and generalized masked diffusion for discrete data. *Advances in neural information processing systems*, 37: 103131–103167, 2024.
- Jascha Sohl-Dickstein, Eric Weiss, Niru Maheswaranathan, and Surya Ganguli. Deep unsupervised learning using nonequilibrium thermodynamics. In *International conference on machine learning*, pp. 2256–2265. pmlr, 2015.
- Jiaming Song, Chenlin Meng, and Stefano Ermon. Denoising diffusion implicit models. *arXiv* preprint arXiv:2010.02502, 2020.
- Mitchell Stern, Noam Shazeer, and Jakob Uszkoreit. Blockwise parallel decoding for deep autoregressive models. *Advances in Neural Information Processing Systems*, 31, 2018.
- Ilya Tolstikhin, Neil Houlsby, Alexander Kolesnikov, Lucas Beyer, Xiaohua Zhai, Thomas Unterthiner, Jessica Yung, Andreas Peter Steiner, Daniel Keysers, Jakob Uszkoreit, Mario Lucic, and Alexey Dosovitskiy. MLP-mixer: An all-MLP architecture for vision. In A. Beygelzimer, Y. Dauphin, P. Liang, and J. Wortman Vaughan (eds.), *Advances in Neural Information Processing Systems*, 2021. URL https://openreview.net/forum?id=EI2KOXKdnP.
- Ashish Vaswani, Noam Shazeer, Niki Parmar, Jakob Uszkoreit, Llion Jones, Aidan N Gomez, Łukasz Kaiser, and Illia Polosukhin. Attention is all you need. *Advances in neural information processing systems*, 30, 2017.
- Qingyan Wei, Yaojie Zhang, Zhiyuan Liu, Dongrui Liu, and Linfeng Zhang. Accelerating diffusion large language models with slowfast sampling: The three golden principles. *CoRR*, 2025.
- Chengyue Wu, Hao Zhang, Shuchen Xue, Zhijian Liu, Shizhe Diao, Ligeng Zhu, Ping Luo, Song Han, and Enze Xie. Fast-dllm: Training-free acceleration of diffusion llm by enabling kv cache and parallel decoding. *arXiv preprint arXiv:2505.22618*, 2025.
- Jiacheng Ye, Zhihui Xie, Lin Zheng, Jiahui Gao, Zirui Wu, Xin Jiang, Zhenguo Li, and Lingpeng Kong. Dream 7b: Diffusion large language models. *arXiv preprint arXiv:2508.15487*, 2025.
- Wayne Xin Zhao, Kun Zhou, Junyi Li, Tianyi Tang, Xiaolei Wang, Yupeng Hou, Yingqian Min, Beichen Zhang, Junjie Zhang, Zican Dong, Yifan Du, Chen Yang, Yushuo Chen, Zhipeng Chen, Jinhao Jiang, Ruiyang Ren, Yifan Li, Xinyu Tang, Zikang Liu, Peiyu Liu, Jian-Yun Nie, and Ji-Rong Wen. A survey of large language models. *arXiv preprint arXiv:2303.18223*, 2023. URL http://arxiv.org/abs/2303.18223.
- Kaiwen Zheng, Yongxin Chen, Hanzi Mao, Ming-Yu Liu, Jun Zhu, and Qinsheng Zhang. Masked diffusion models are secretly time-agnostic masked models and exploit inaccurate categorical sampling. *arXiv* preprint arXiv:2409.02908, 2024.
- Kun Zhou, Yifan Li, Wayne Xin Zhao, and Ji rong Wen. Diffusion-nat: Self-prompting discrete diffusion for non-autoregressive text generation. In *Conference of the European Chapter of the Association for Computational Linguistics*, 2023. URL https://api.semanticscholar.org/CorpusID:258557887.

Zhuang Ziyu, Chen Qiguang, Ma Longxuan, Li Mingda, Han Yi, Qian Yushan, Bai Haopeng, Zhang Weinan, and Ting Liu. Through the lens of core competency: Survey on evaluation of large language models. In Jiajun Zhang (ed.), *Proceedings of the 22nd Chinese National Conference on Computational Linguistics (Volume 2: Frontier Forum)*, pp. 88–109, Harbin, China, August 2023. Chinese Information Processing Society of China. URL https://aclanthology.org/2023.ccl-2.8/.

# A THE USE OF LARGE LANGUAGE MODELS

Large language models (LLMs) were used in this work exclusively for the purpose of text polishing and refinement. Their role was strictly limited to assisting with grammatical correction, improving sentence fluency, and enhancing word choice to increase the overall clarity and readability of the manuscript.

## B UPDATE INFERENCE ALGORITHM

#### Algorithm 3 Update Inference

702

703 704

705

706

708 709

710 711 712

713

714

715

716

717

718

719

720

721

722

723

724

725

726

727

728

729

730

731 732 733

734

747

748

749

750

751

752

753

754

755

```
Require: Diffusion large language model M, filter model f_{\theta}, prompt set x_{\text{prompt}}, generation length
     L_{\rm gen}, block size s, filter threshold \tau
 1: for each x_i \in x_{\text{prompt}} do
          l_i \leftarrow length(x_i), X \leftarrow concat(x_i, [MASK]^{L_{gen}})
 2:
          for b=0,...,\frac{L_{\mathrm{gen}}}{c}-1 do
 3:
                \mathcal{M} \leftarrow \{1, 2, ..., s\}
 4:
 5:
                while \mathcal{M} \neq \emptyset do
 6:
                     con f_t, pre_t = M(X), logit_t = f_{\theta}(con f_t)
 7:
                     if logit_{t,j} > \tau then
 8:
                          \mathcal{M} \leftarrow \mathcal{M} \setminus \{j\}, X_{i+b\cdot s+j} \leftarrow pre_{t,j}
 9:
                     end if
                end while
10:
11:
                if [endoftext] in X then
12:
                     break
13:
               end if
          end for
14:
15:
          response_i = X_{l_i:l_i+L_{gen}-1}
16: end for
17: return response
```

# C EXPERIMENTS AND ANALYSIS ON EOTP MECHANISM

Table 5: A comparison of LLaDA and EoTP mechanisms in different generation lengths.

Methods	Generation Length	TPS	Speed	Score
	256	3.41	1.00×	78.70
LLaDA	512	1.67	1.00×	77.71
	1024	0.54	1.00×	77.62
	256	3.76	1.10×	79.23
+ EoTP	512	3.38	$2.02 \times$	78.77
	1024	3.25	$5.98 \times$	79.38

This table 5 clearly demonstrates the significant advantage of integrating the EoTP mechanism with the base LLaDA model, particularly for long-sequence generation. While the standalone LLaDA model exhibits substantial performance degradation as generation length increases—evidenced by the sharp decline in TPS from 3.41 to 0.54—the incorporation of EoTP not only mitigates this degradation but also delivers considerable speedup. Most notably, at a sequence length of 1024, EoTP achieves a dramatic 5.98× acceleration while simultaneously improving output quality, with the Score increasing from 77.62 to 79.38. These gains can be largely attributed to the elimination of redundant computation: quantitative analysis shows that 89.59% of the baseline computational cost arises from decoding padding tokens after the [EoT] token. EoTP effectively removes this overhead by dynamically detecting sequence completion once all original non-[MASK] positions are unmasked, thereby optimizing inference efficiency without compromising performance.

# D TRAINING CURVE OF FILTER MODEL

As shown in Figure 7, this learning curve illustrates that both training (blue) and validation (red) loss fall sharply in the earliest epochs (from 0.68 to 0.28), then decrease much more gradually over the full 5,000-epoch run, approaching a plateau near 0.21–0.23. The validation curve remains slightly above the training curve throughout, indicating only a modest generalization gap rather than pronounced overfitting; the parallel, steady decline shows the model continues to improve on unseen data but with diminishing returns. The long, flat tail of both curves indicates the model has effectively converged.

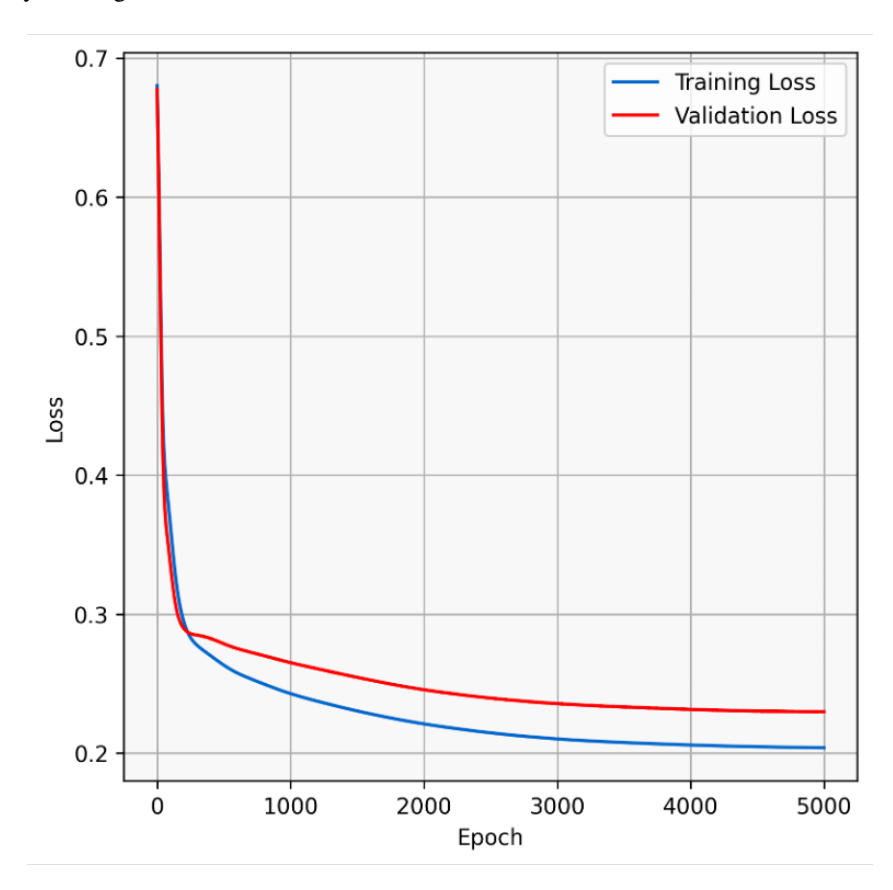


Figure 7: Learning curve of filter model  $f_{\theta}$ . The learning curves illustrate the progression of training and validation loss across 5,000 epochs, with the former in blue and the latter in red.